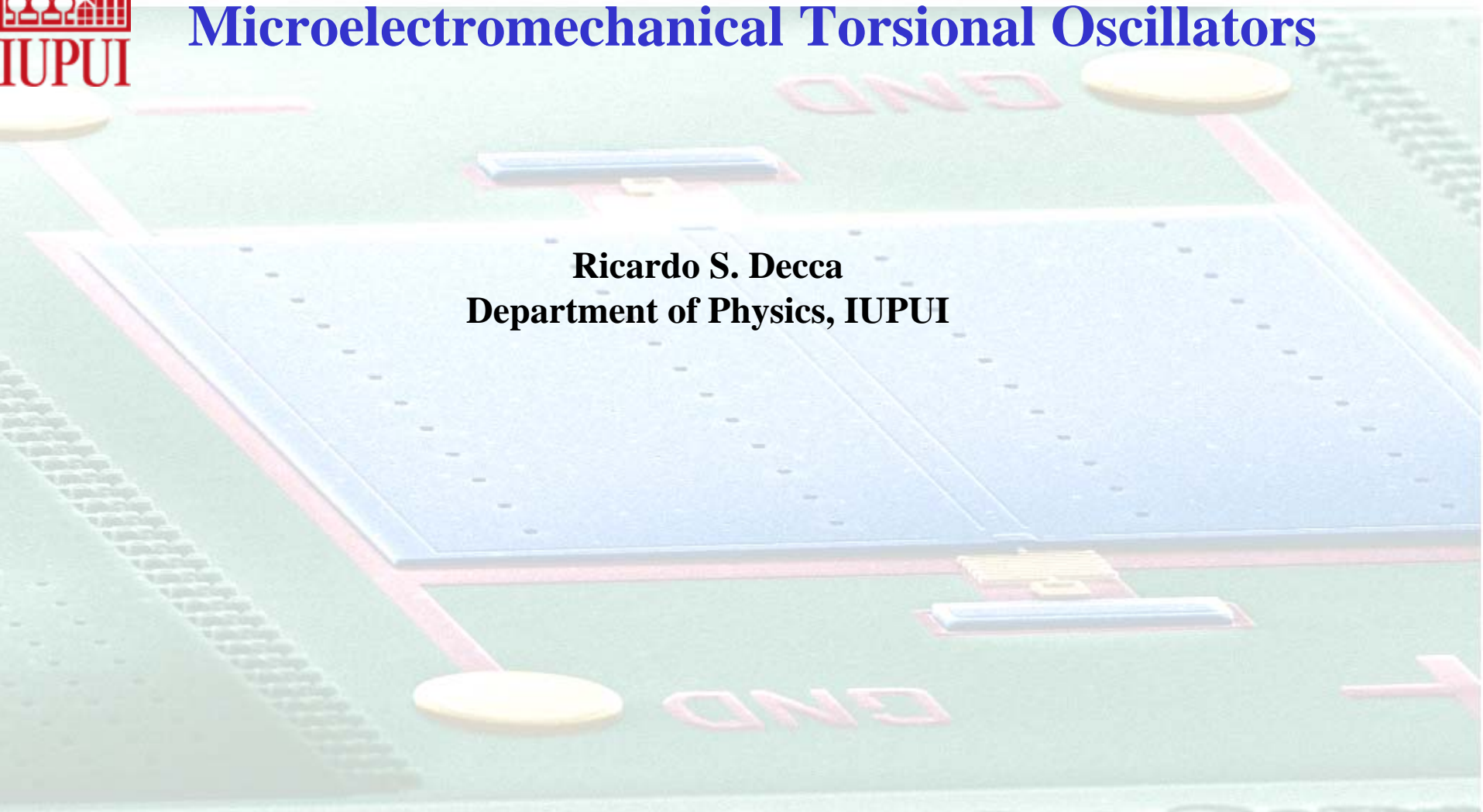




Precise Measurements of the Casimir Force using Microelectromechanical Torsional Oscillators

Ricardo S. Decca
Department of Physics, IUPUI



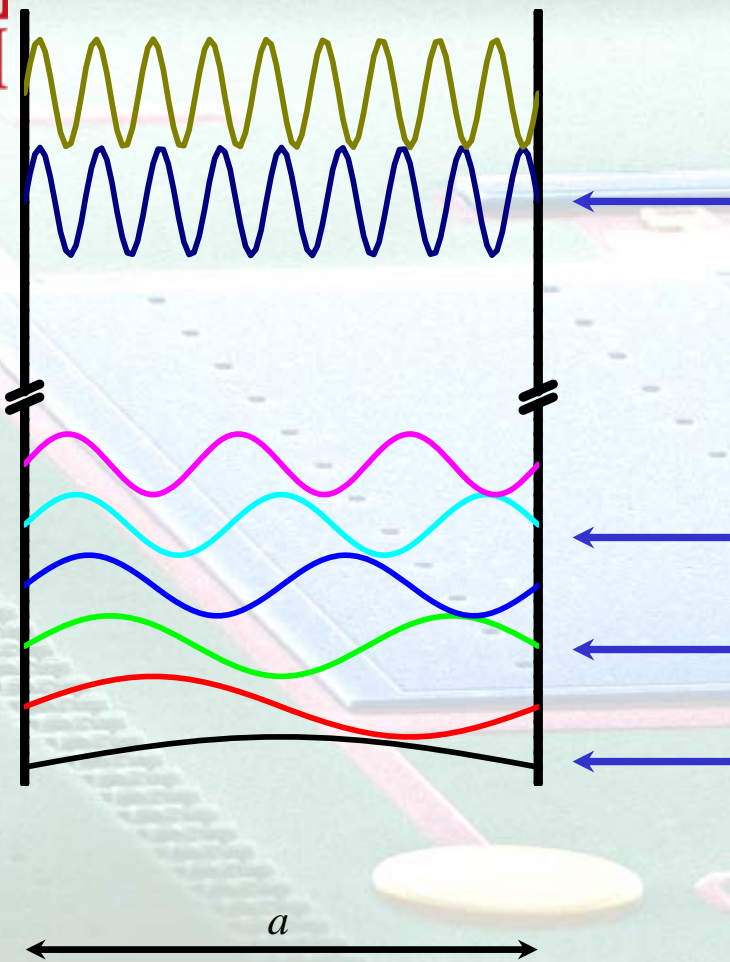


Collaborators

Daniel López	Alcatel-Lucent Technologies (currently at Argonne National Labs)
Ephraim Fischbasch	Purdue University
Dennis E. Krausse	Wabash College and Purdue University
Valdimir M. Mostepanenko	Noncommercial Partnership “Scientific Instruments”, Russia
Galina L. Klimchitskaya	North-West Technical University, Russia
Eduardo Osquiguil	Instituto Balseiro, Argentina. Fullbright Fellow.
Jing Ding	IUPUI

Funding

NSF, DOE, LANL



$$\langle 0 | \mathbf{E} | 0 \rangle = \langle 0 | \mathbf{B} | 0 \rangle = 0$$

$$\frac{1}{2} \langle 0 | (\mathbf{E}^2 + \mathbf{B}^2) | 0 \rangle = \langle 0 | \mathbf{E}^2 | 0 \rangle = \frac{1}{2\Omega} \sum_{\omega, \mathbf{k}} \omega_k$$

$$P_C = -\frac{\pi \hbar c}{480 a^4}$$

Vacuum fluctuations plus boundaries

Same result when using the Lifshitz approach

- Dominant electronic force at small (~ 1 nm) separations
- Non-retarded: van der Waals
- Retarded: Casimir

No mode restriction on the outside



Importance of the Casimir effect

- **Consequences in nanotechnology (MEMS and NEMS)**
 - “Long-range” interaction between moving parts
 - Possibility of controlling the interaction by engineering materials
- **Consequences in quantum field theory**
 - Thermal dependence
- **Consequences in gravitation and cosmology**
 - Background to measure deviations from Newtonian potential at small separations

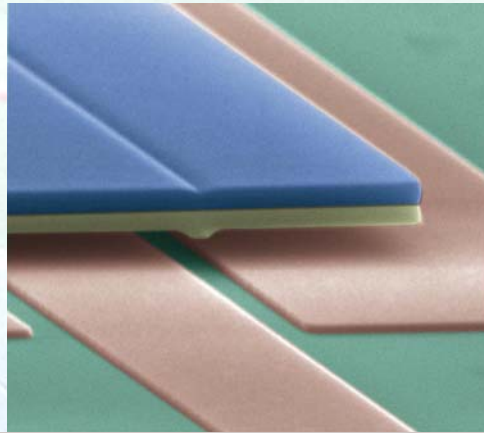


Outline

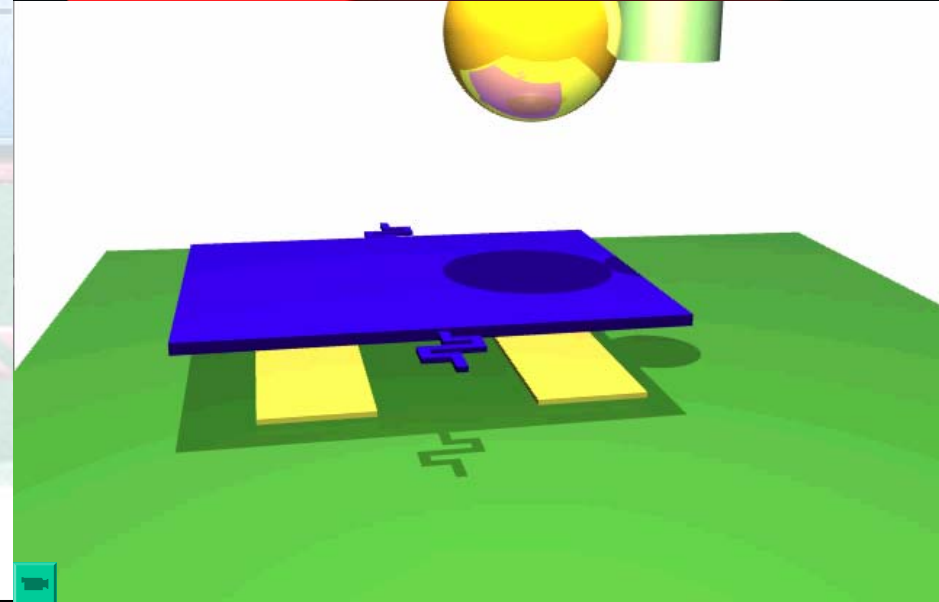
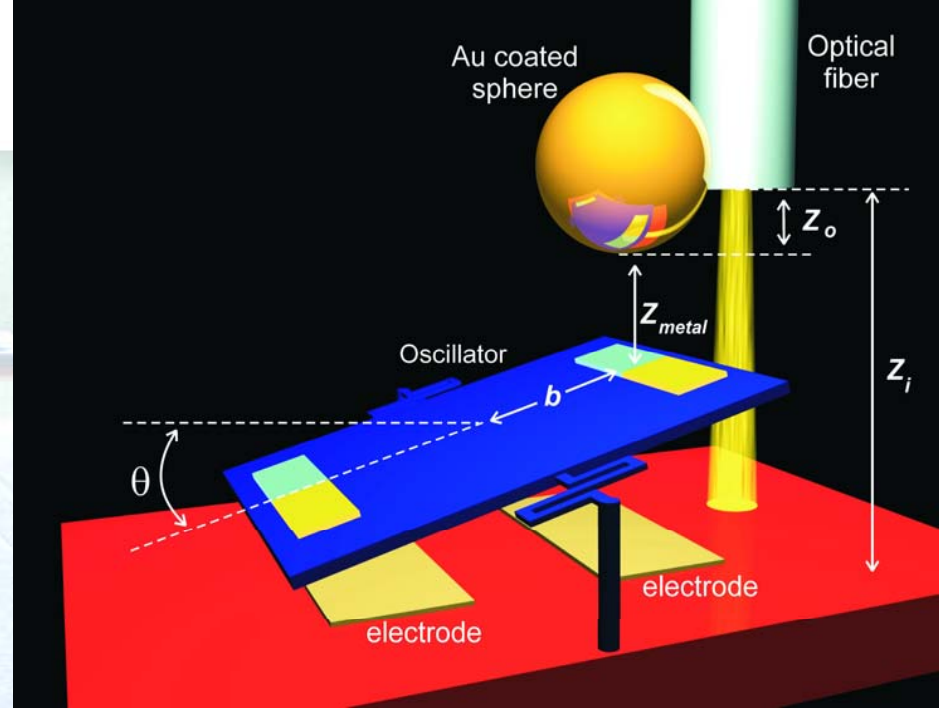
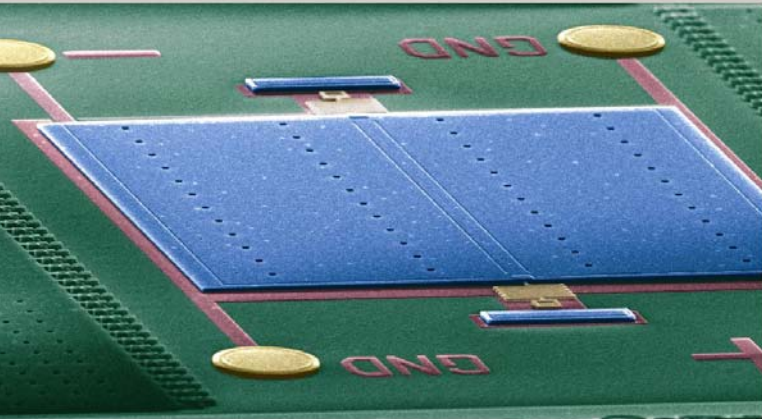
- **Precise measurements of the Casimir force**
 - Experimental setup
 - Minimum detectable force
 - Position separation
 - Calibrations
 - Error budget
 - Comparison with theory
- **Low temperature measurements**
 - Experimental setup
 - Incomplete results
- **Proximity force approximation**
 - An experimentalist view of the PFA
- **Summary**



Experimental setup

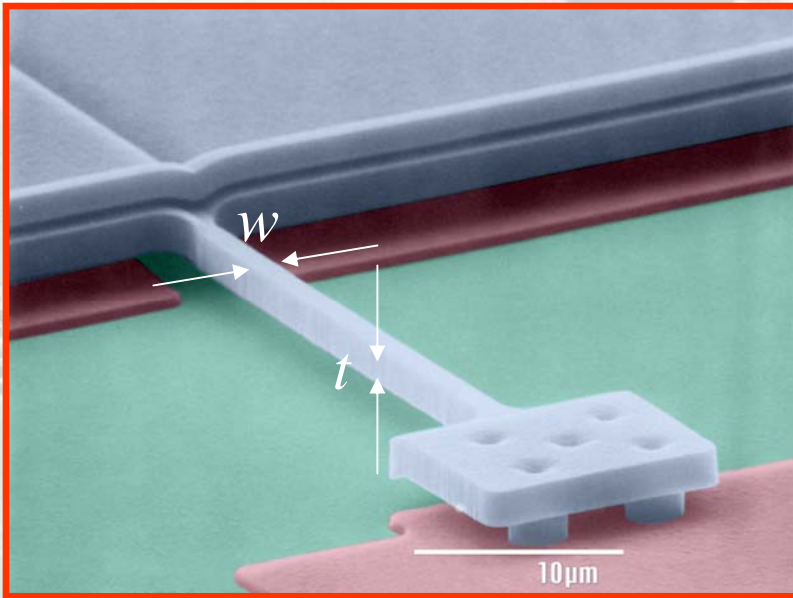


$$z_{metal} = z_i - z_o - z_g - b \Theta$$

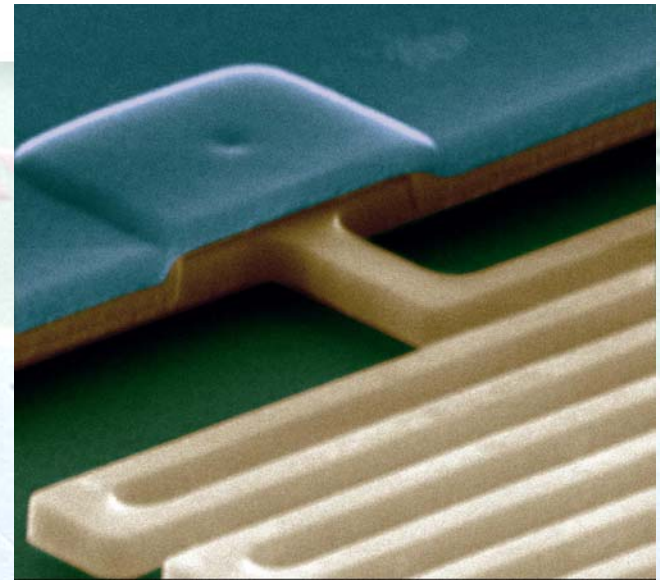


Experimental setup

$$\delta F = \sqrt{\frac{(2k_B T \kappa)}{\pi f_r Q}} \frac{1}{b}$$



$w, t = 2\mu\text{m}$



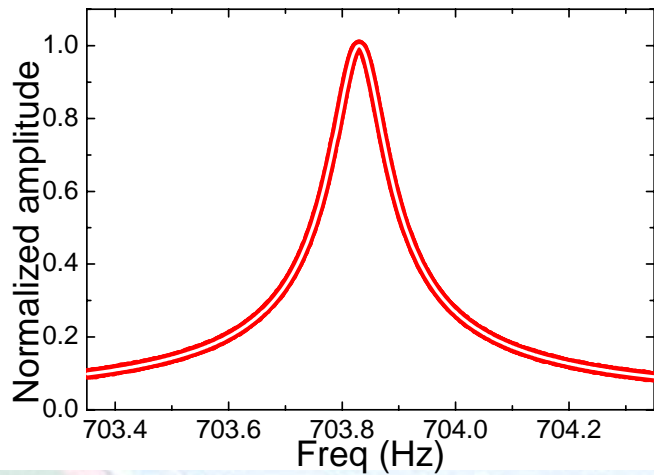
$$\kappa_s = \frac{wt^3 E_{Si}}{6L_{serp}} \sim 9 \times 10^{-10} \frac{Nm}{rad}$$

$$\kappa_r \approx \frac{2w^3 t E_{Si}}{3L}$$

$$\kappa_s \approx \kappa_r / 40$$

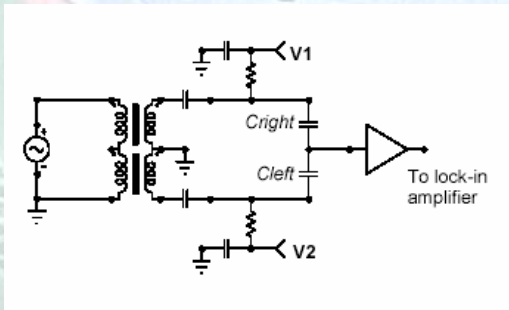


Minimum detectable force

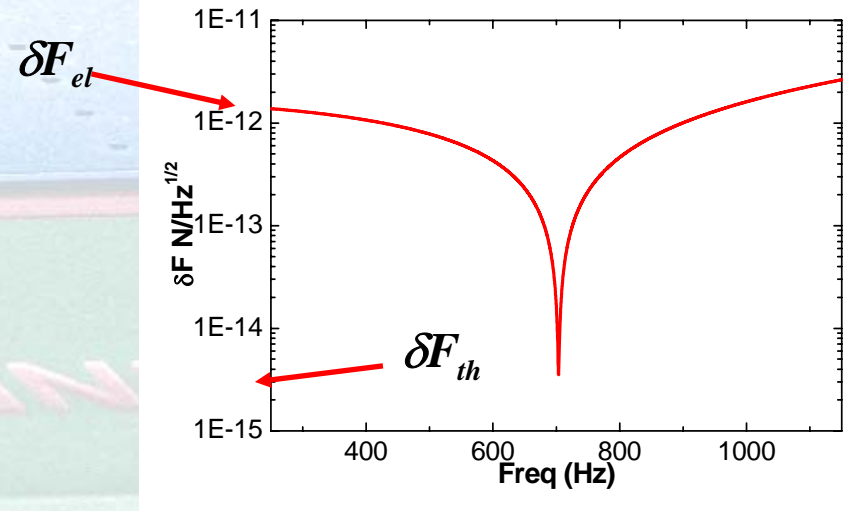


$$\delta F = \frac{1}{b} \sqrt{\left(\frac{4k_B T \kappa}{\omega_o Q}\right)^2 + \left(\frac{\delta \theta_{el} \kappa}{A(\omega)}\right)^2}$$

$$= \frac{1}{b} \sqrt{\delta F_{th}^2 + \delta F_{el}^2} \sim 4 \text{ fN} / \sqrt{\text{Hz}}$$



$$\delta \theta \approx 10^{-9} \text{ rad} / \sqrt{\text{Hz}}$$

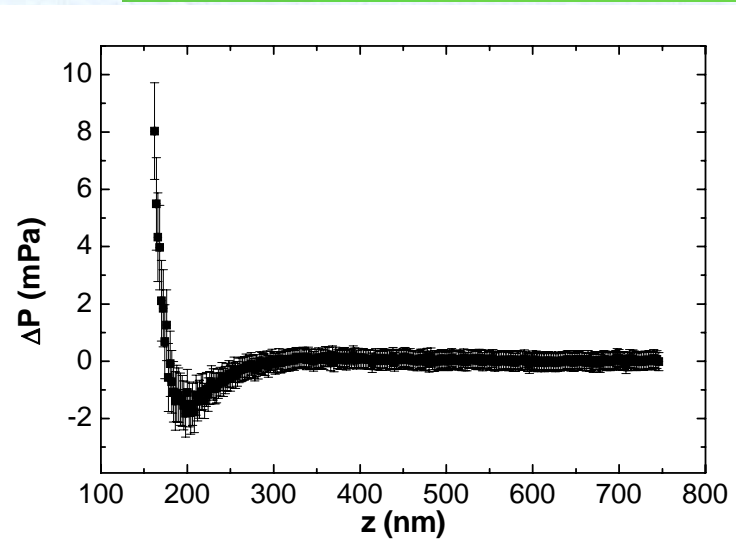
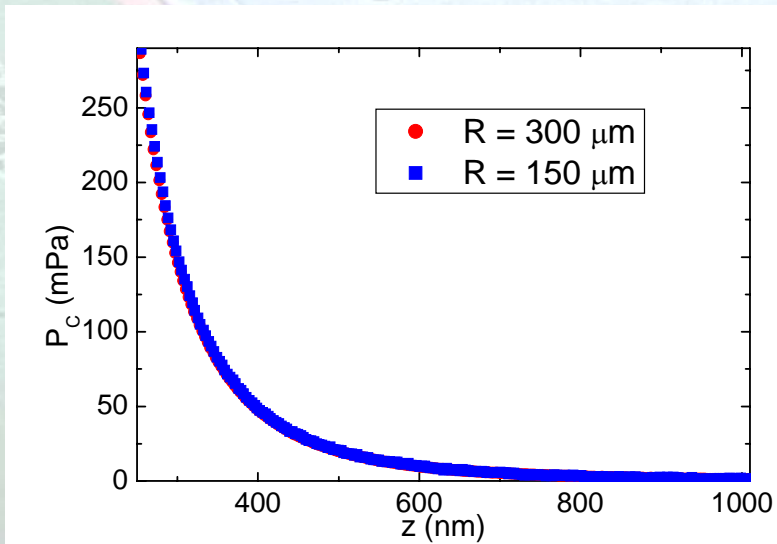
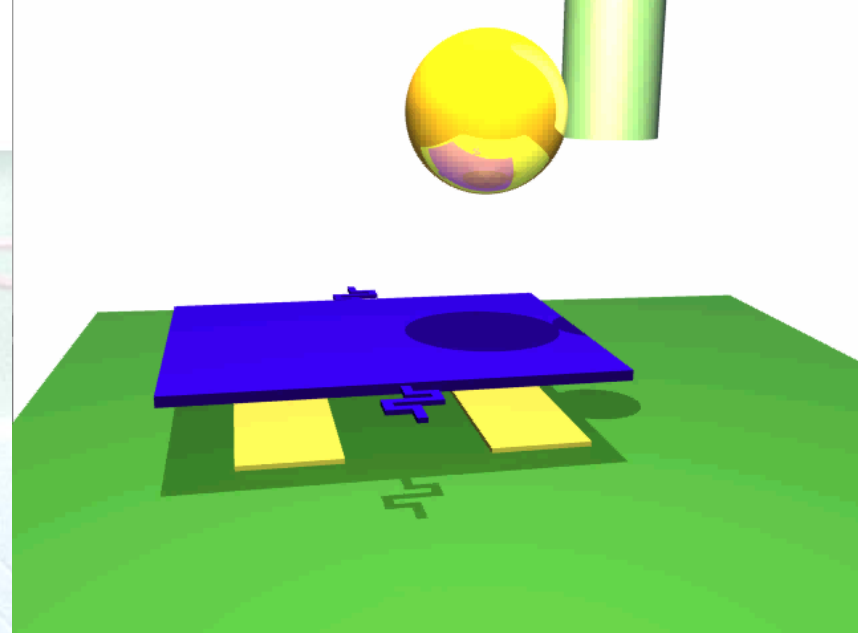




Dynamic measurements

$$\omega_r^2 = \omega_o^2 \left(1 - \frac{b^2}{I\omega_o^2} \frac{\partial F_C}{\partial z} \right)$$

$$F_C = 2\pi R \times E_C \Rightarrow \frac{\partial F_C}{\partial z} = 2\pi R \times P_C$$



Separation measurement

z_o is determined using a known interaction

z_i, Θ are measured for each position

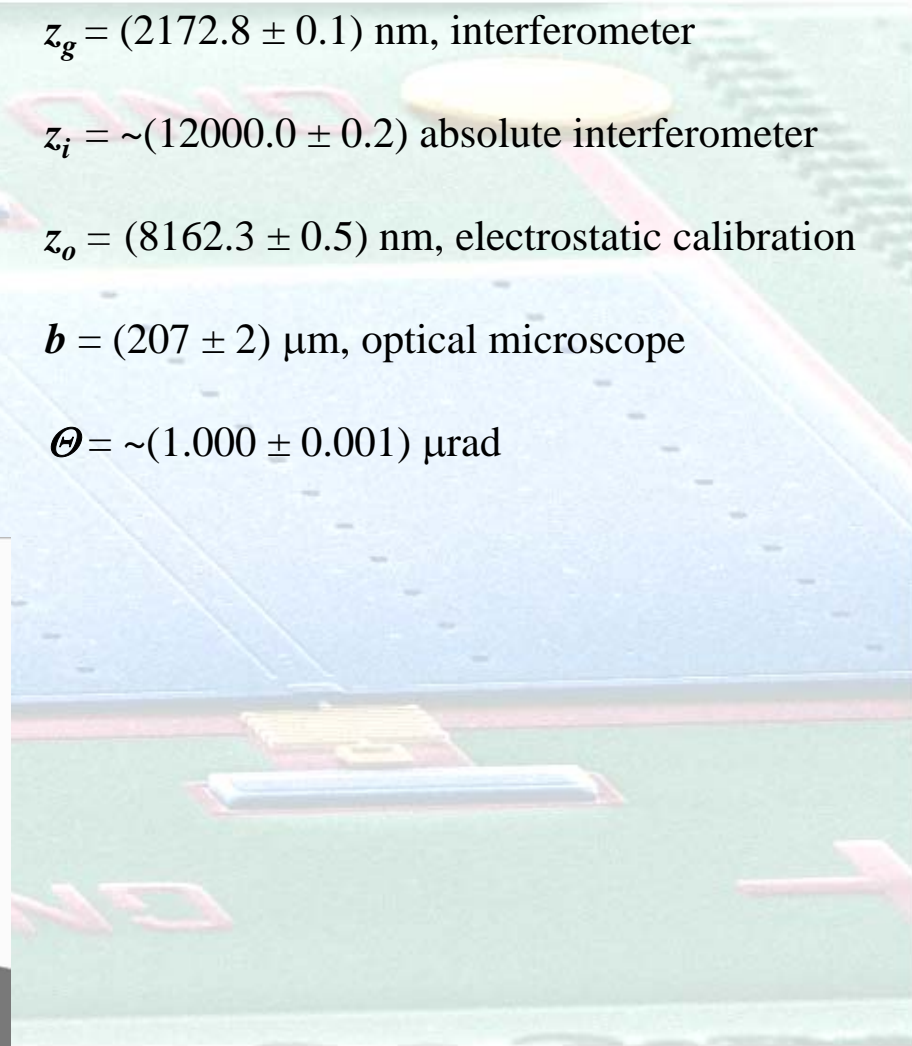
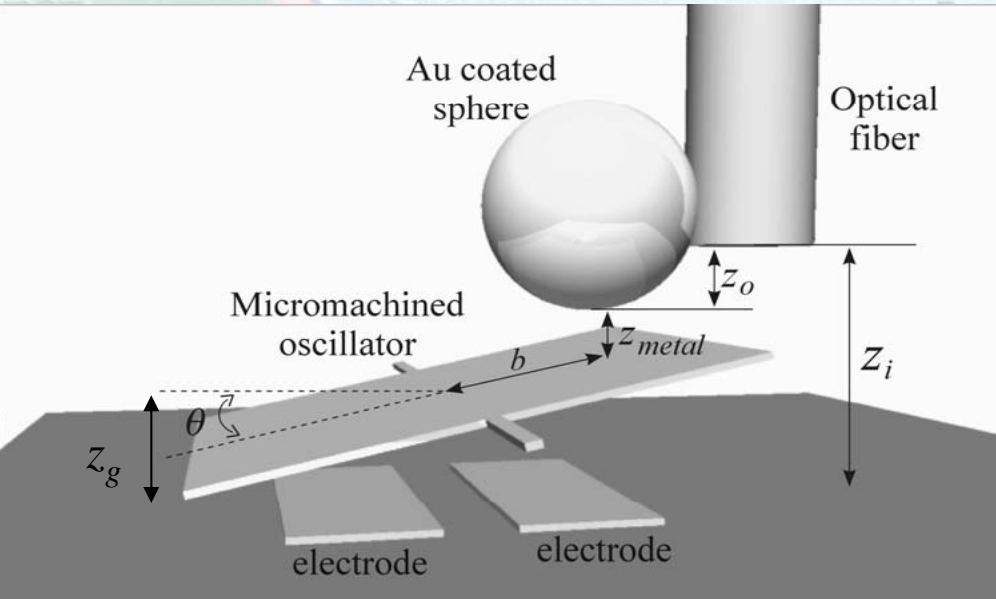
$z_g = (2172.8 \pm 0.1)$ nm, interferometer

$z_i = \sim(12000.0 \pm 0.2)$ absolute interferometer

$z_o = (8162.3 \pm 0.5)$ nm, electrostatic calibration

$b = (207 \pm 2)$ μ m, optical microscope

$\Theta = \sim(1.000 \pm 0.001)$ μ rad





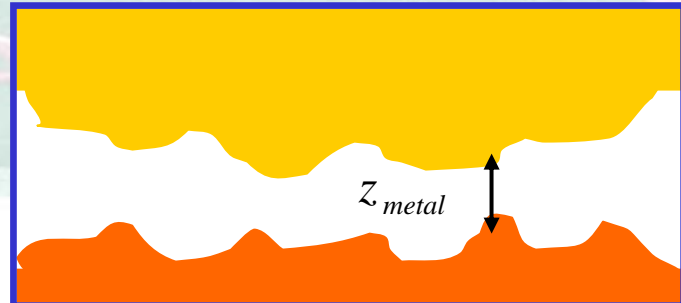
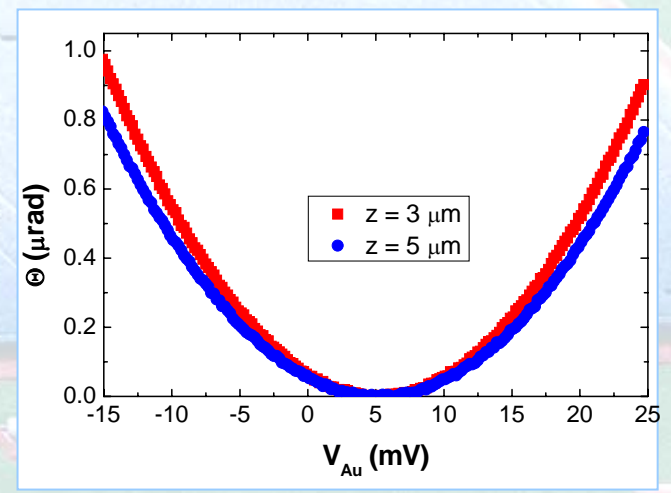
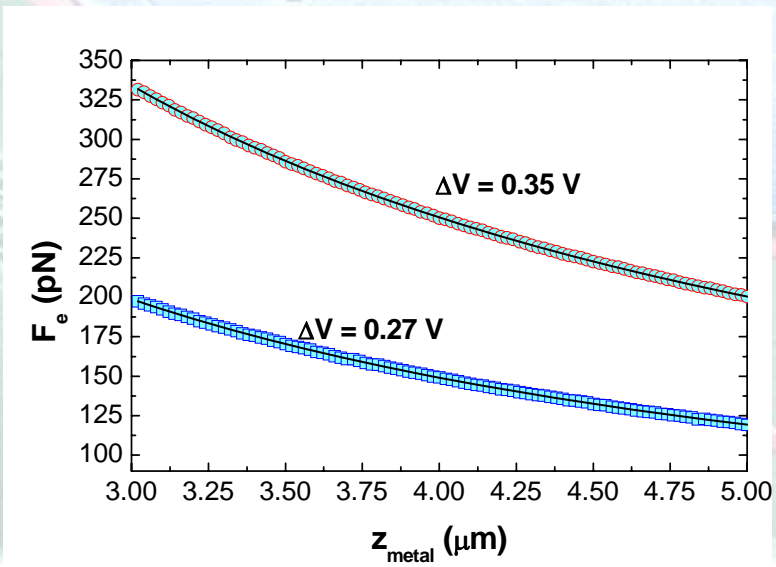
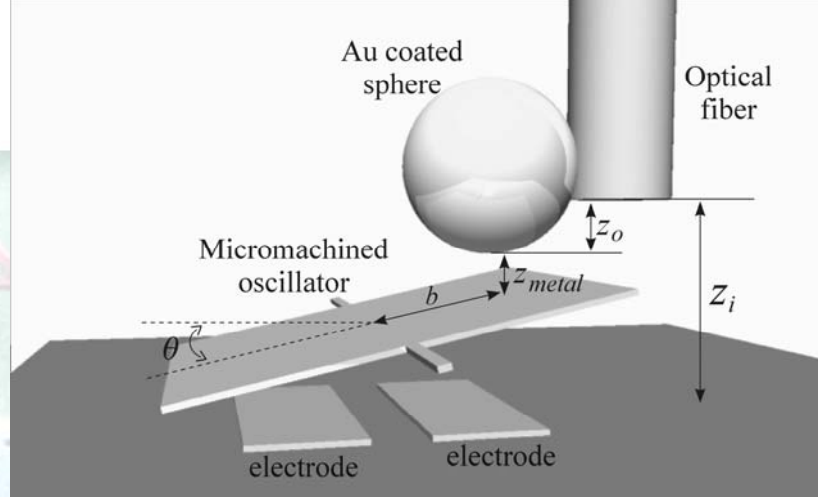
Separation measurement

Electrostatic force calibration

$$F_e = -2\pi\epsilon_o (V - V_{Au})^2 \sum_n \frac{\coth u - n \coth nu}{\sinh nu} \sim$$

$$-2\pi\epsilon_o (V - V_{Au})^2 \sum_{i=0} A_i \left(\frac{R}{(z_{metal} + \bar{z})} \right)^{1-i}$$

$$u = 1 + \frac{(z_{metal} + \bar{z})}{R}$$

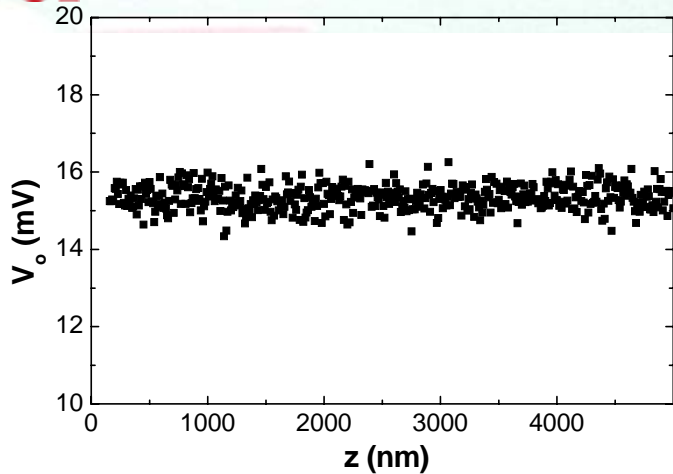




Separation measurement

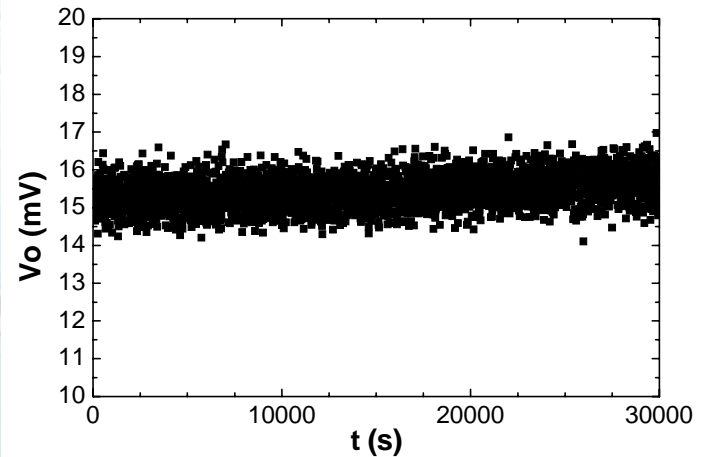
IUPUI

Electrostatic force calibration



V_0 must be constant as a function of separation...

... and time



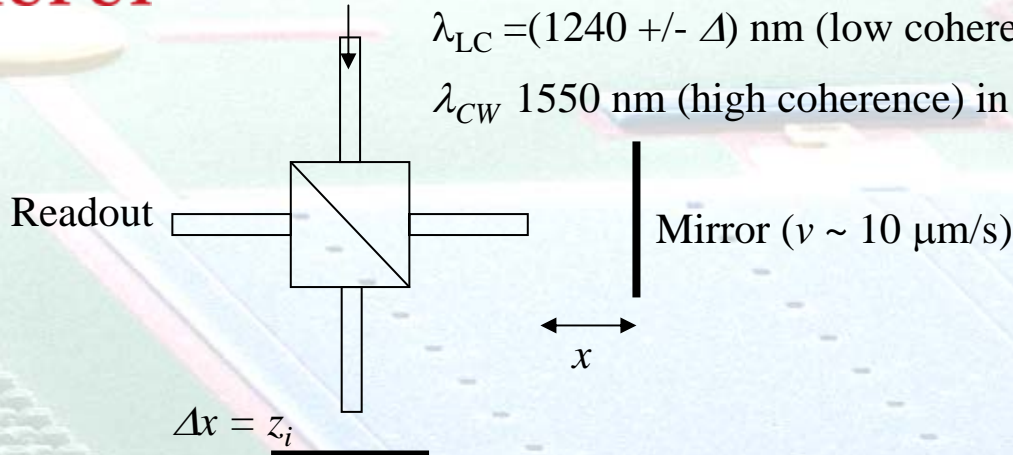
Otherwise, V_0 needs to be determined at each point



Distance measurement

Interferometer (Yang *et al.*, Opt. Lett. **27**, 77 (2005))

$\lambda_{LC} = (1240 \pm \Delta)$ nm (low coherence),
 λ_{CW} 1550 nm (high coherence) in



$$\psi_D = \psi_{LC} - \frac{4}{5} \psi_{CW}$$

$$z_i = \frac{\lambda_{CW}}{4} [\text{int}(S_{fringe}) + S_{phase}]$$

$$S_{phase} = (\psi_D(x_1) - \psi_D(x_2)) \pmod{2\pi}$$

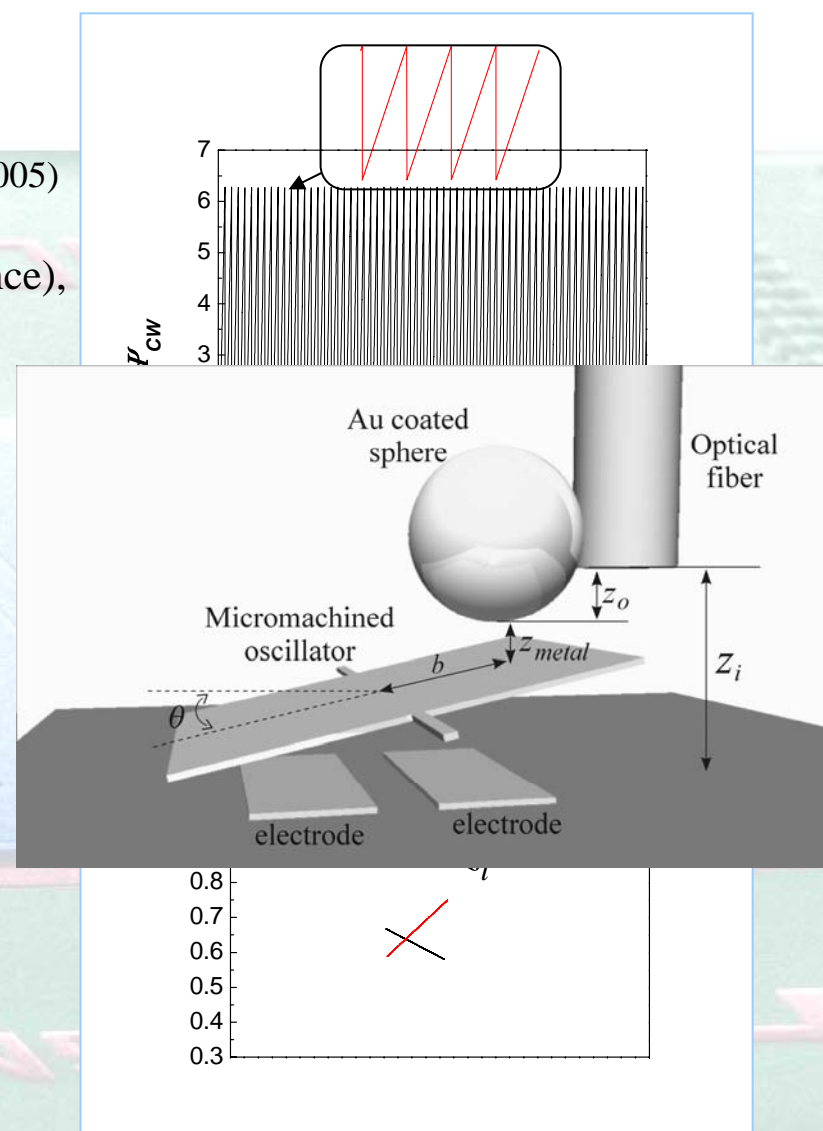
-Phases obtained doing a Hilbert transform of the amplitude

-Changes in Δ (about 2 nm) give different curves.

Intersections provide Δx

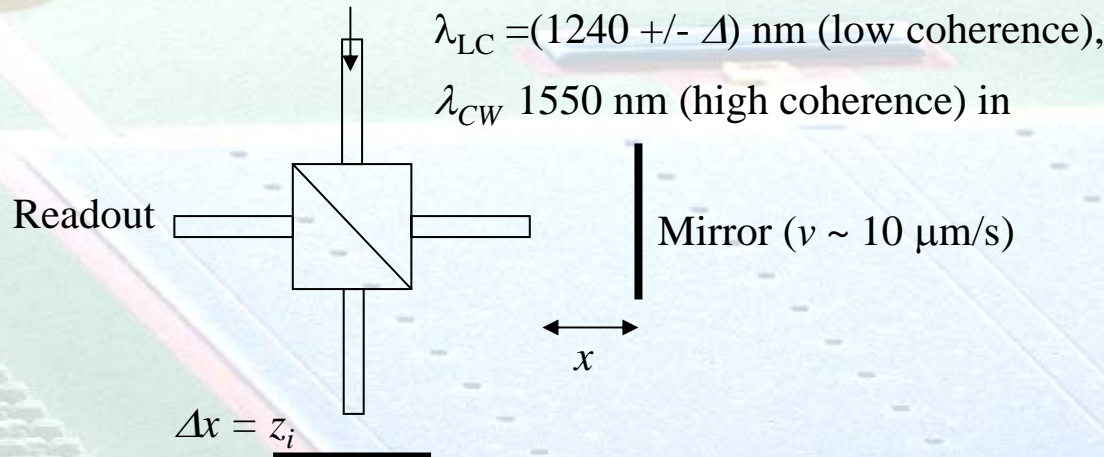
-Quite insensitive to jitter. Only $2\Delta\Delta x' / (\lambda_{CW})^2$

Instead of $2\Delta x' / \lambda_{CW}$



Distance measurement

Interferometer (Yang *et al.*, Opt. Lett. **27**, 77 (2005))



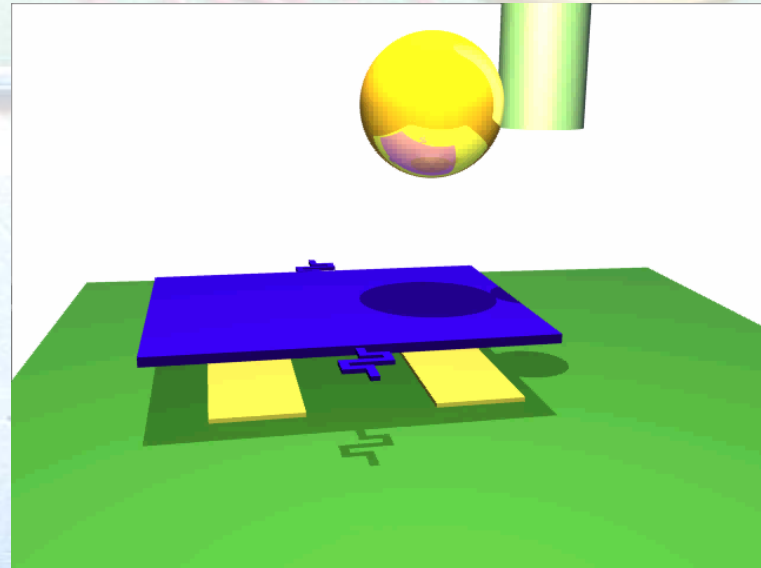
-Problems in lack of parallelism (curvature of wavefronts) are compensated when subtracting the two phases

-Gouy phase effect is $\sim \phi_G(\omega) \cong \arctan\left(\frac{\Delta f}{NA \cdot f}\right)$, and gives an error much smaller than the random one

Pressure determination

Three effects:

- New equilibrium position
- Softer spring
- Non-linear effects





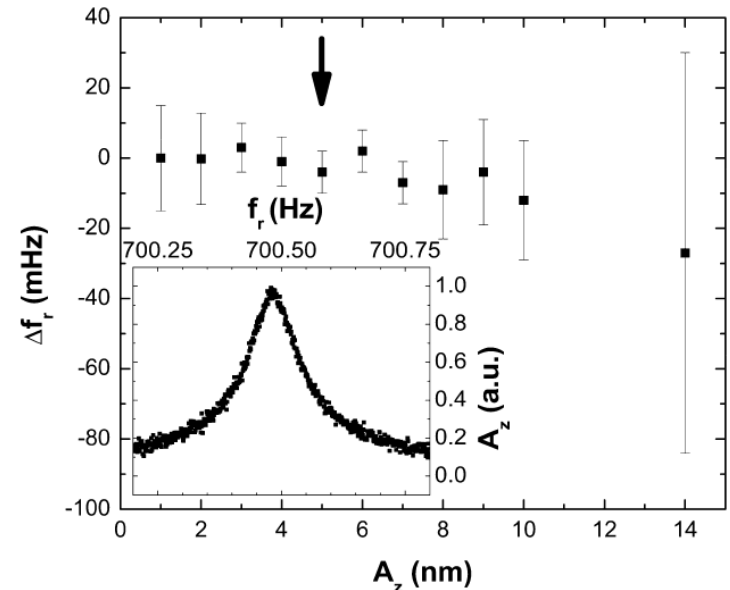
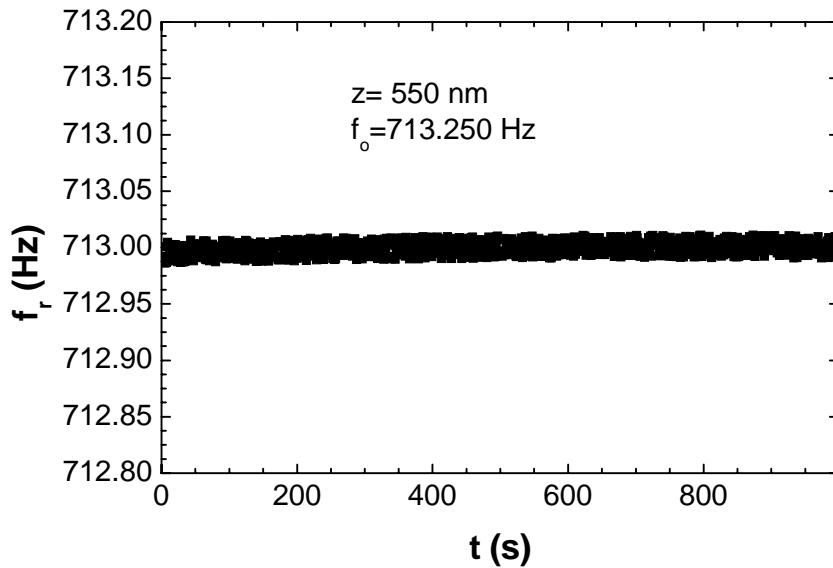
Pressure determination

$$\omega_r^2 = \omega_o^2 \left(1 - \frac{b^2}{I\omega_o^2} \frac{\partial F_C}{\partial z} \right)$$

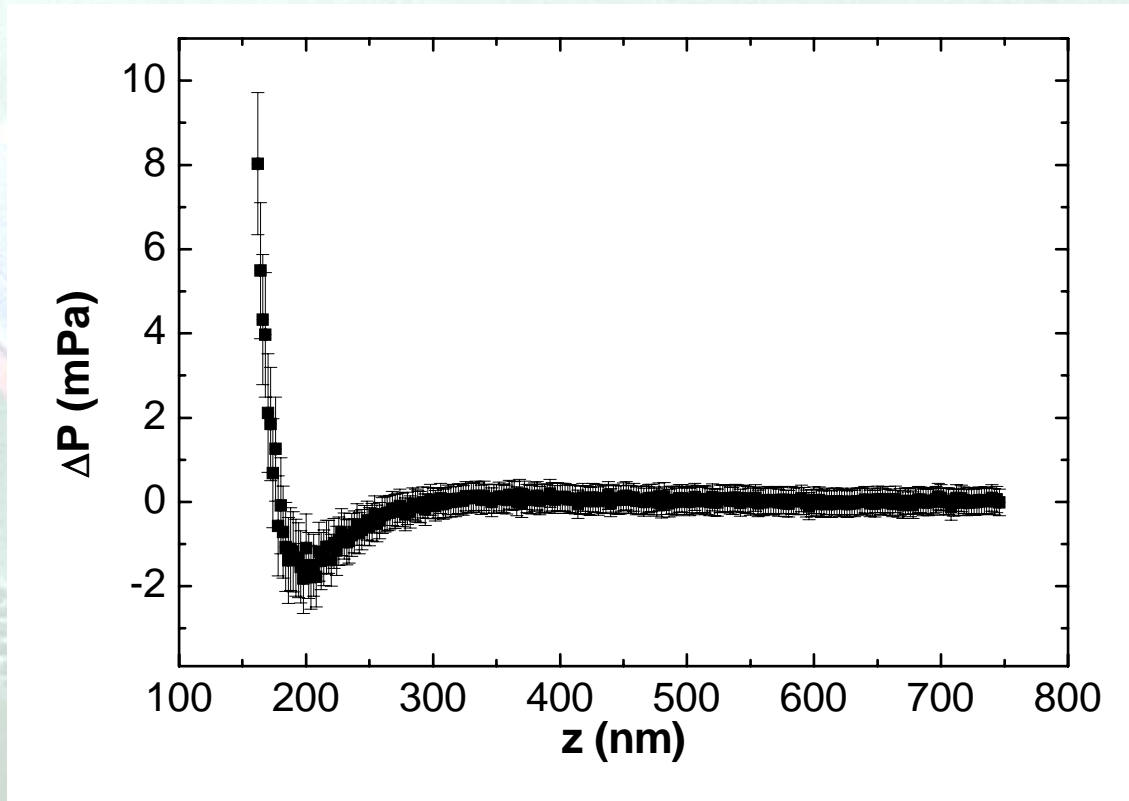
$$F_C = 2\pi R \times E_C \Rightarrow \frac{\partial F_C}{\partial z} = 2\pi R \times P_C$$

Determined by:

- looking into the response of the oscillator in the thermal bath
- Inducing a time dependent separation between the plate and the sphere

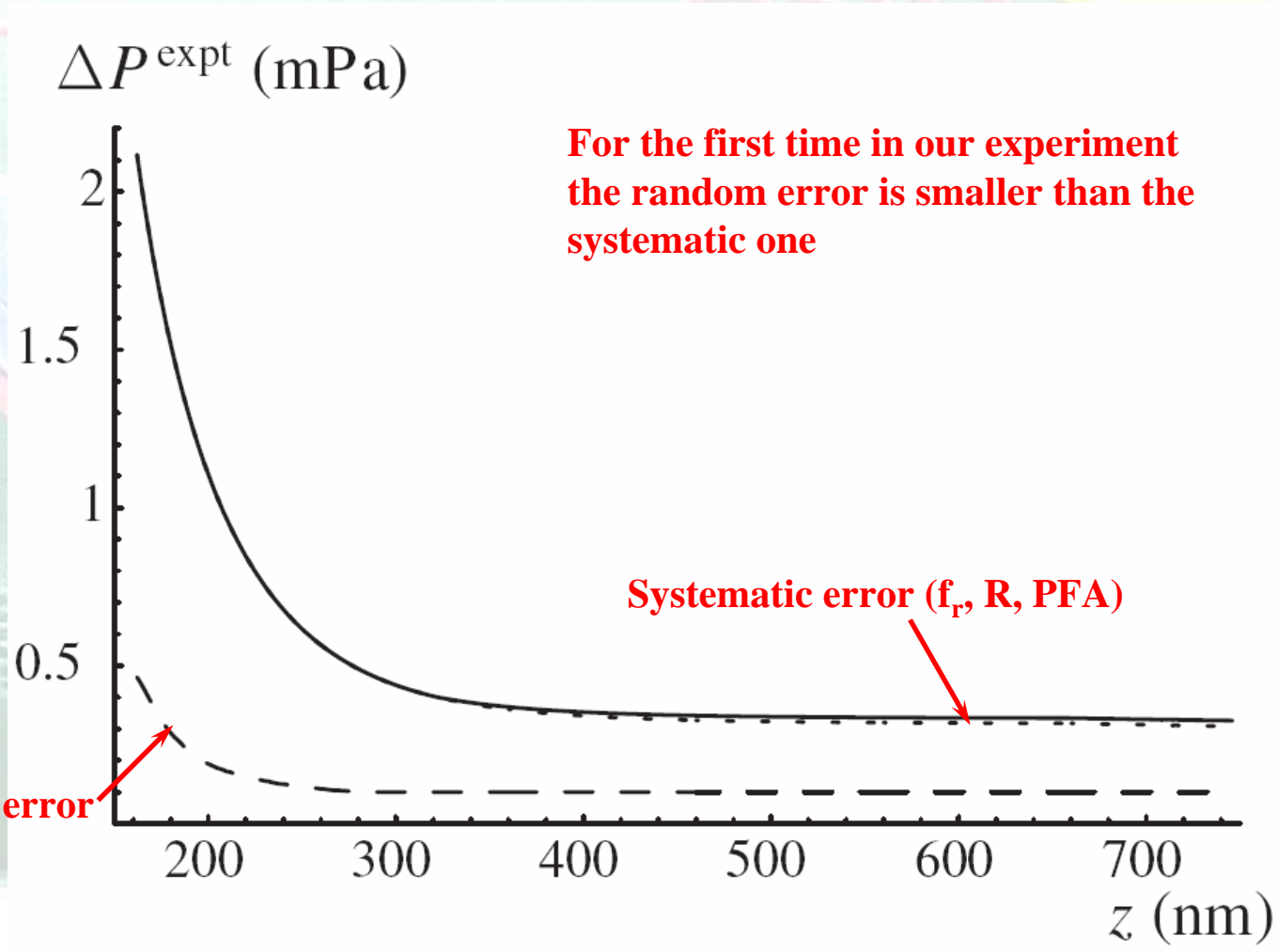


Equivalent P_C measurement





Error budget



**For the first time in our experiment
the random error is smaller than the
systematic one**

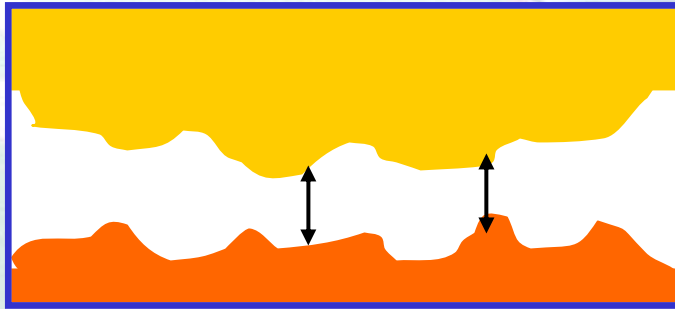
Random error

Systematic error (f_r, R, PFA)



Comparison with theory

Roughness corrections

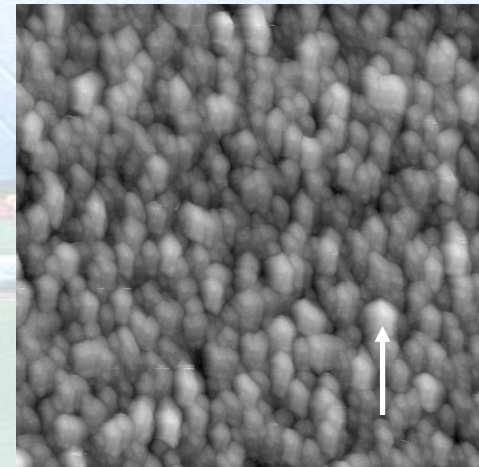
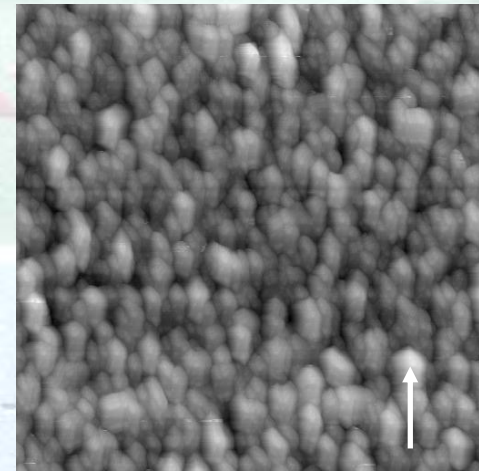


$$F_C = \sum_i v_i F_{CS}(z_i)$$

v_i : Fraction of the sample at separation z_i

Roughness corrections are ~0.5% to the Casimir force at 160 nm

AFM image of the Au plane



(10x10 μm^2)
~ 20 nm_{pp}



Comparison with theory

IUPUI

Finite conductivity and finite temperature

$$P(z) = -\frac{k_B T}{\pi} \sum_{l=0}^{\infty} \int_0^{\infty} k_{\perp} dk_{\perp} q_l \times \left\{ [r_{\parallel}^{-2}(\xi_l, k_{\perp}) e^{2q_l z} - 1]^{-1} + [r_{\perp}^{-2}(\xi_l, k_{\perp}) e^{2q_l z} - 1]^{-1} \right\}$$

$$r_{\parallel, L}^{-2}(\xi_l, k_{\perp}) = \left[\frac{k_l + \varepsilon(i\xi_l) q_l}{k_l - \varepsilon(i\xi_l) q_l} \right]^2, \quad r_{\perp, L}^{-2}(\xi_l, k_{\perp}) = \left[\frac{k_l + q_l}{k_l - q_l} \right]^2$$

$$q_l^2 = k_{\perp}^2 + \left(\frac{4\pi^2 k_B T l}{hc} \right)^2$$

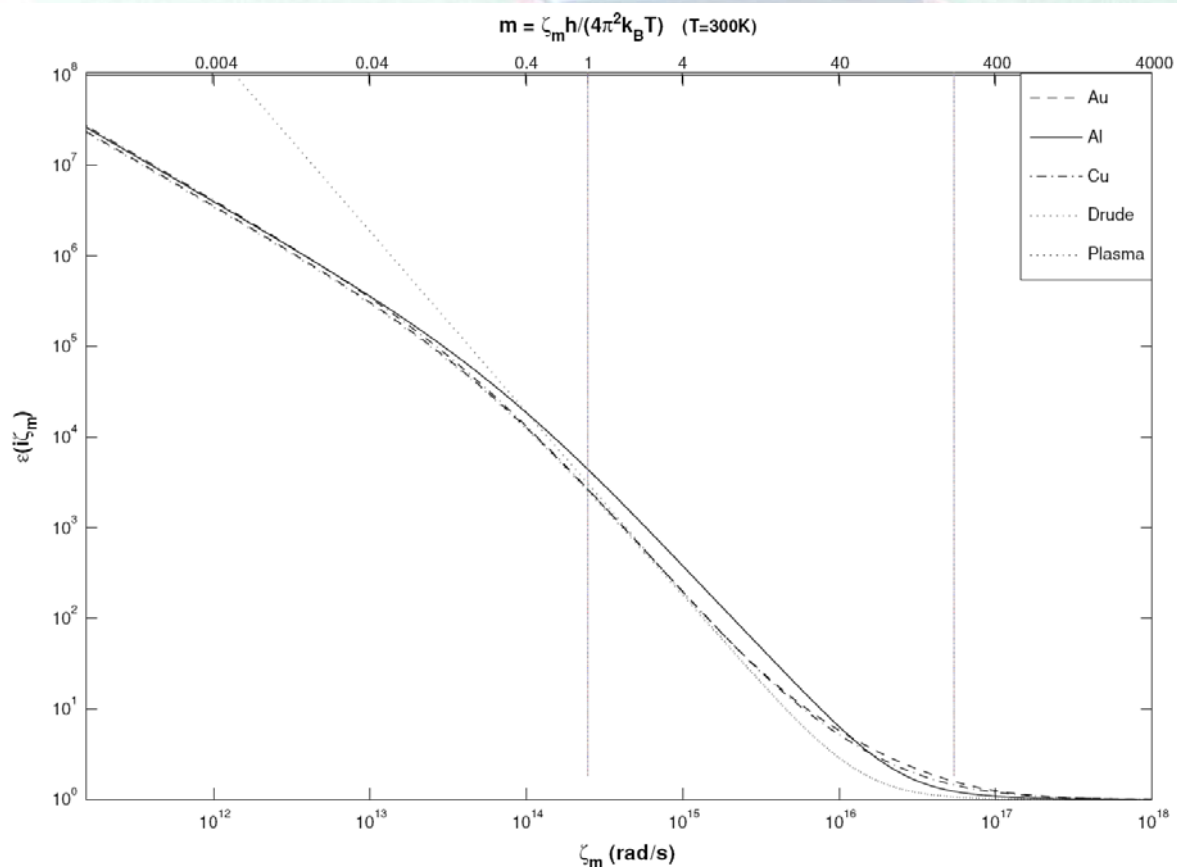
$$\varepsilon(i\xi) = 1 + \frac{2}{\pi} \int_0^{\infty} \frac{\omega \operatorname{Im} \varepsilon(\omega)}{\omega^2 + \xi^2} d\omega$$

$$k_l^2 = k_{\perp}^2 + \varepsilon(i\xi_l) \xi_l^2 / c^2$$



Comparison with theory

$$\epsilon(i\xi) = 1 + \frac{2}{\pi} \int_0^\infty \frac{\omega \text{Im} \epsilon(\omega)}{\omega^2 + \xi^2} d\omega$$



$$\epsilon(\omega) = 1 - \frac{\omega_p^2}{\omega(\omega + i\gamma)}$$

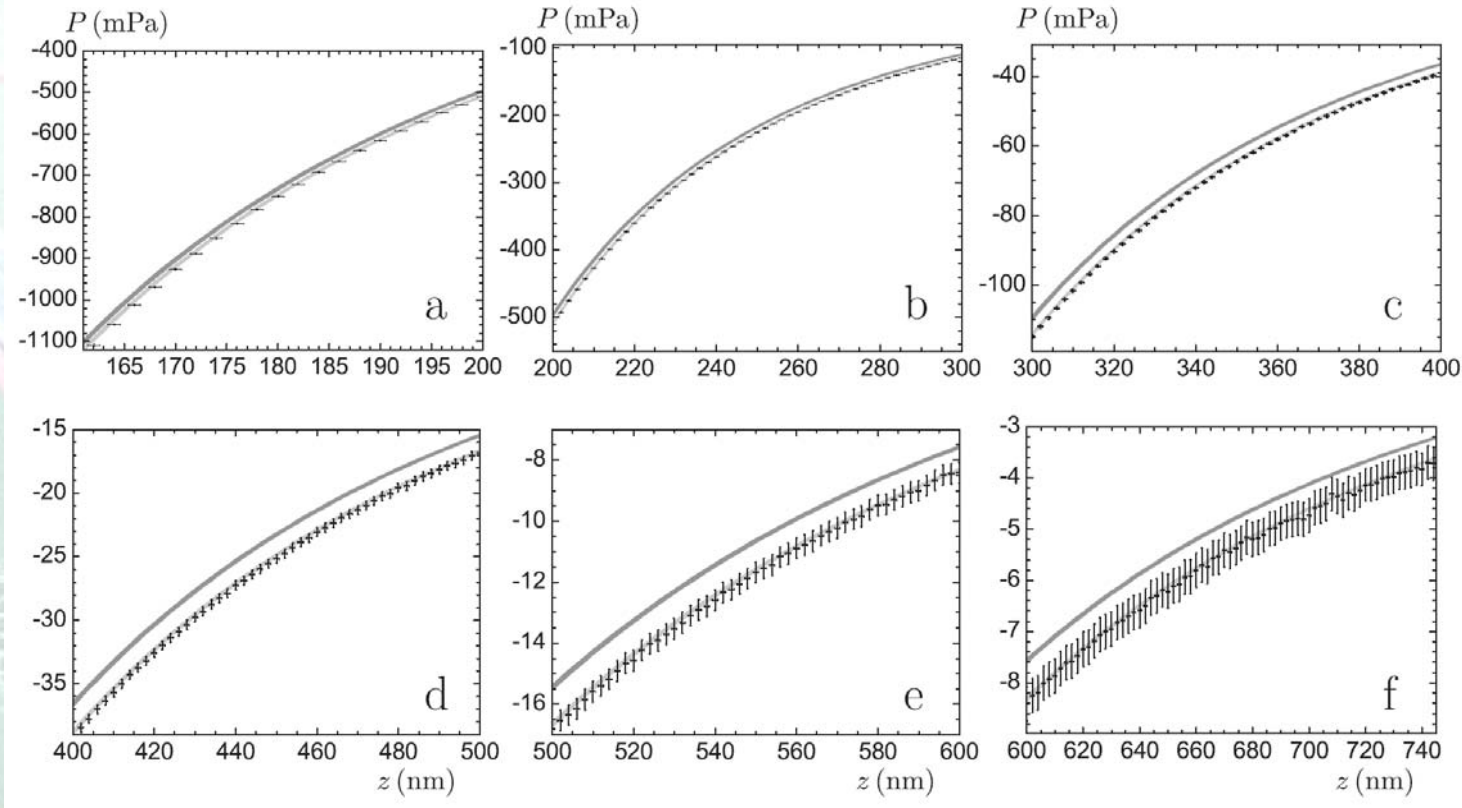
$$\epsilon(\omega) = 1 - \frac{\omega_p^2}{\omega^2}$$

Bentsen et al., J. Phys. A (2005)



Pressure determination

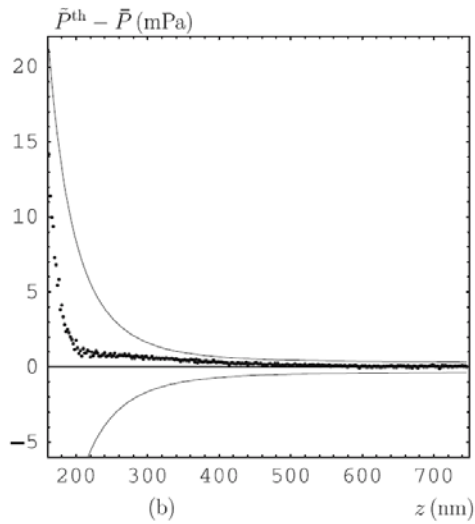
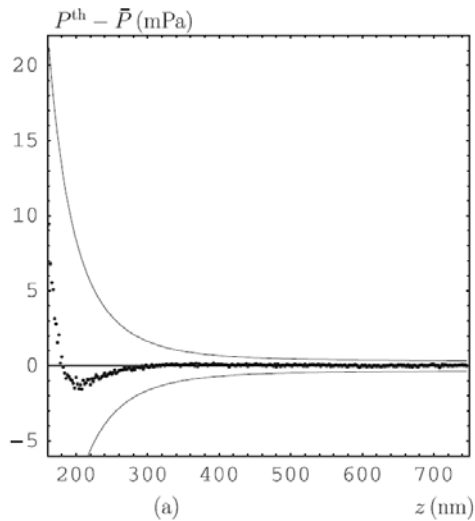
PRD 75, 077101



- Dark grey, Drude model approach
- Light grey, impedance approach

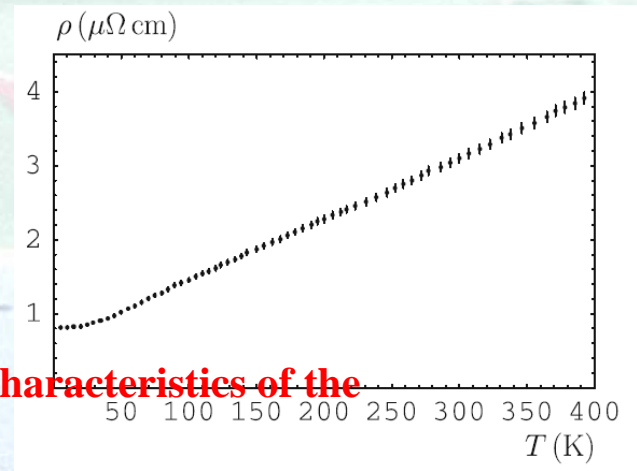


Pressure determination



Plasma model

What are the characteristics of the Au used?

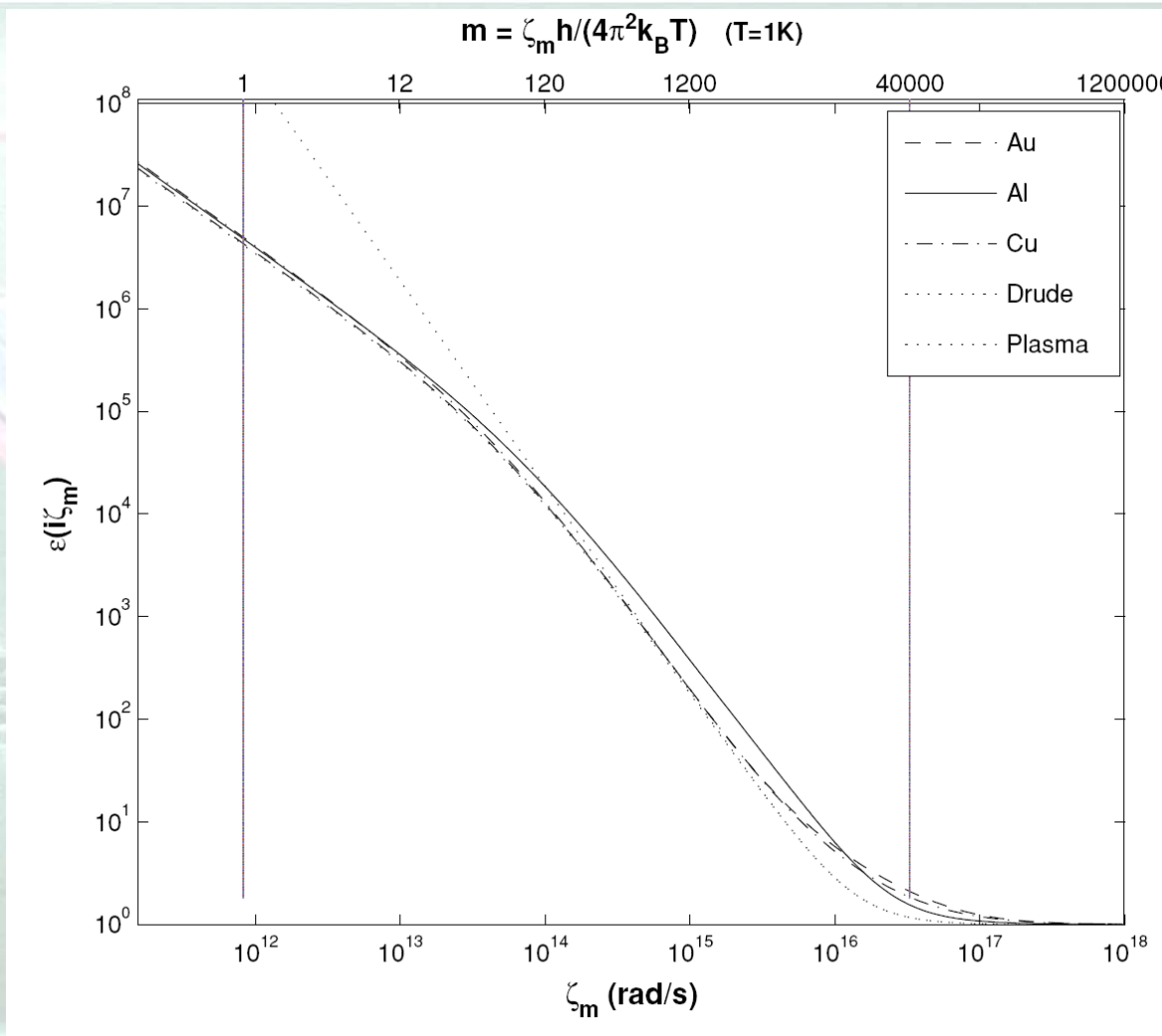


$$\rho(T) = \frac{4\pi}{\omega_p^2 \cdot \tau(T)} \propto \frac{T}{\omega_p^{3/2}}$$

Leontovich impedance $\omega_p = (8.9 \pm 0.1)eV$



Low temperature measurement

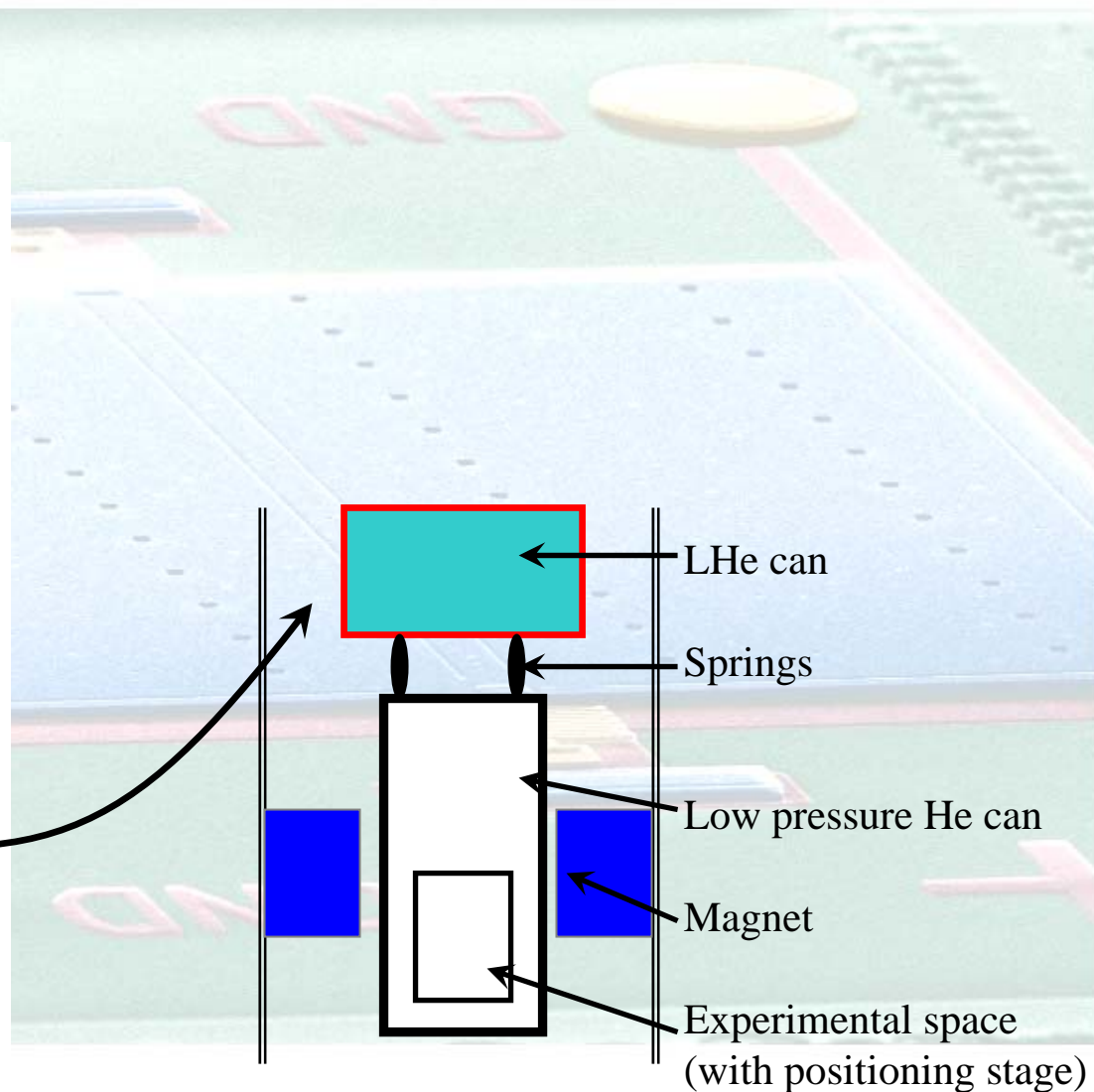
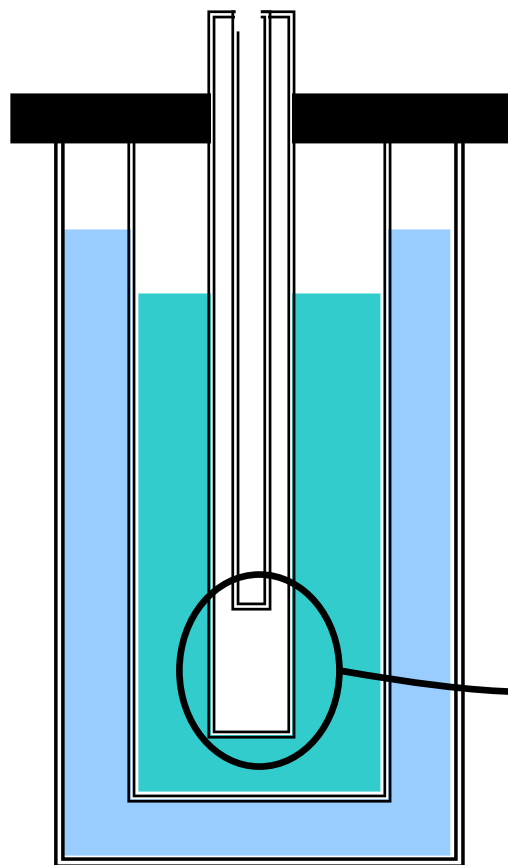




IUPUI

Low temperature measurement

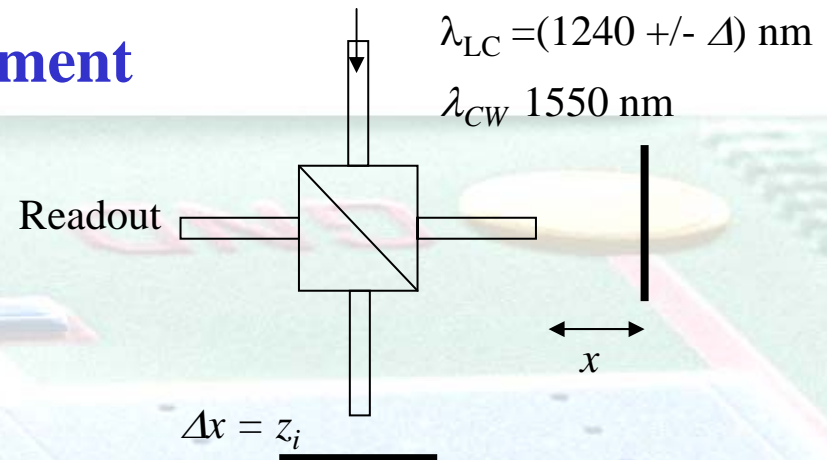
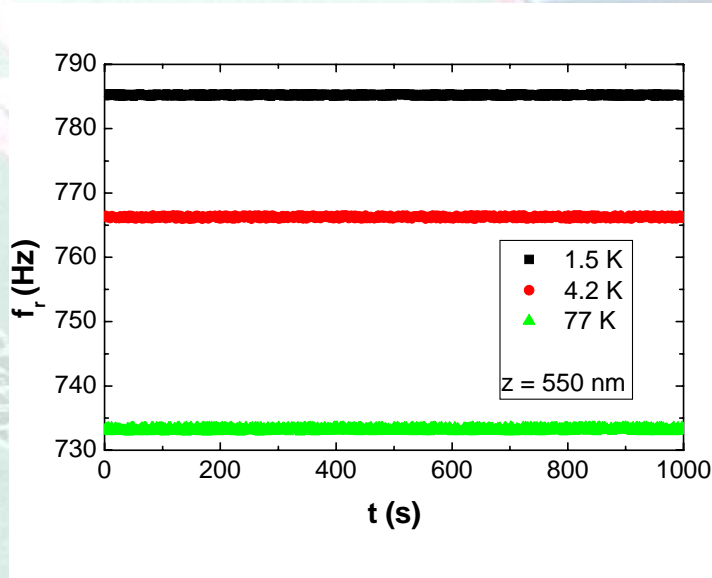
Setup schematic





Low temperature measurement

Characterization



Measured error is ~ 5 nm.

Mechanical vibrations

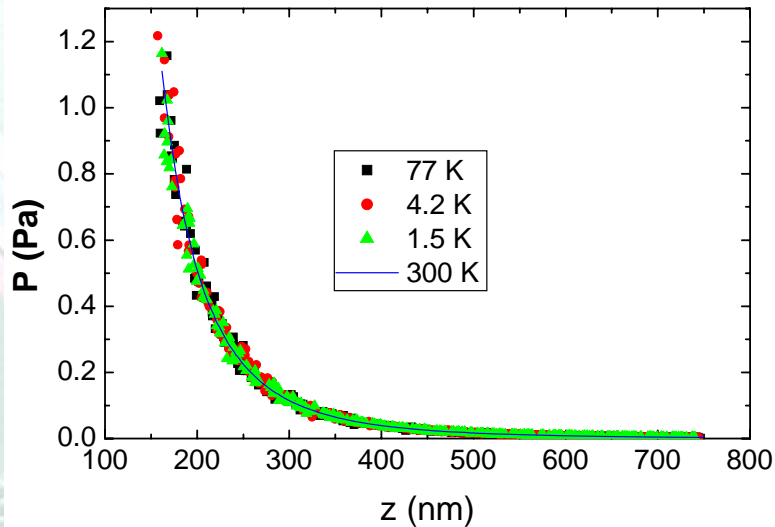
and problems with the interferometer

When compared with previous measurements, the error in frequency is ~ 30 times larger at 1.5 K and ~ 40 times larger at 4.2 K and 77 K, yielding an increased error in P_C



Low temperature measurement

Results



Measurements at 1.5 K have the lowest noise

All data seem to coincide with the room temperature measurements within the larger Experimental errors

The error on the low T measurement, $e_l(400 \text{ nm}) = 5 \text{ mPa}$ is larger than the difference between the Drude and plasma models of 2.4 mPa

This statement holds true at all temperatures and separations investigated



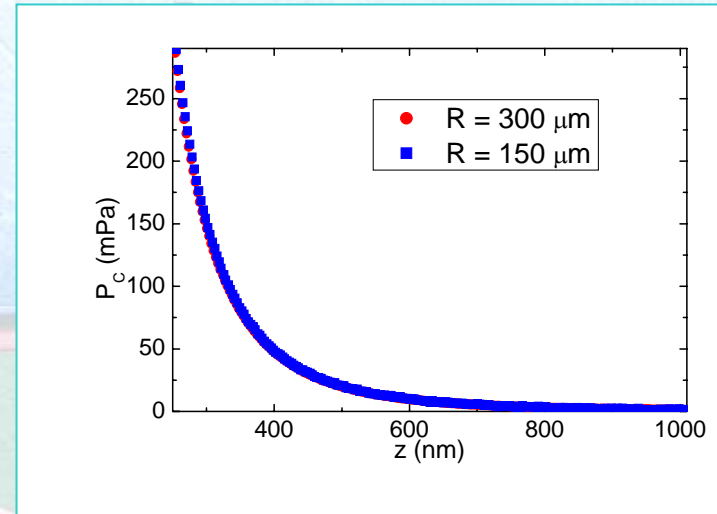
Proximity force approximation

$$F_C(z, R) = 2\pi R \times \varepsilon_{Casimir}^{pp}(z) \left[1 + \beta \frac{z}{R} + \dots \right]$$

$$P^{eff}(z, R) = P^{pp}(z) \left[1 + \beta' \frac{z}{R} + \dots \right] = -\frac{1}{2\pi R} \frac{\partial F_C}{\partial z}$$

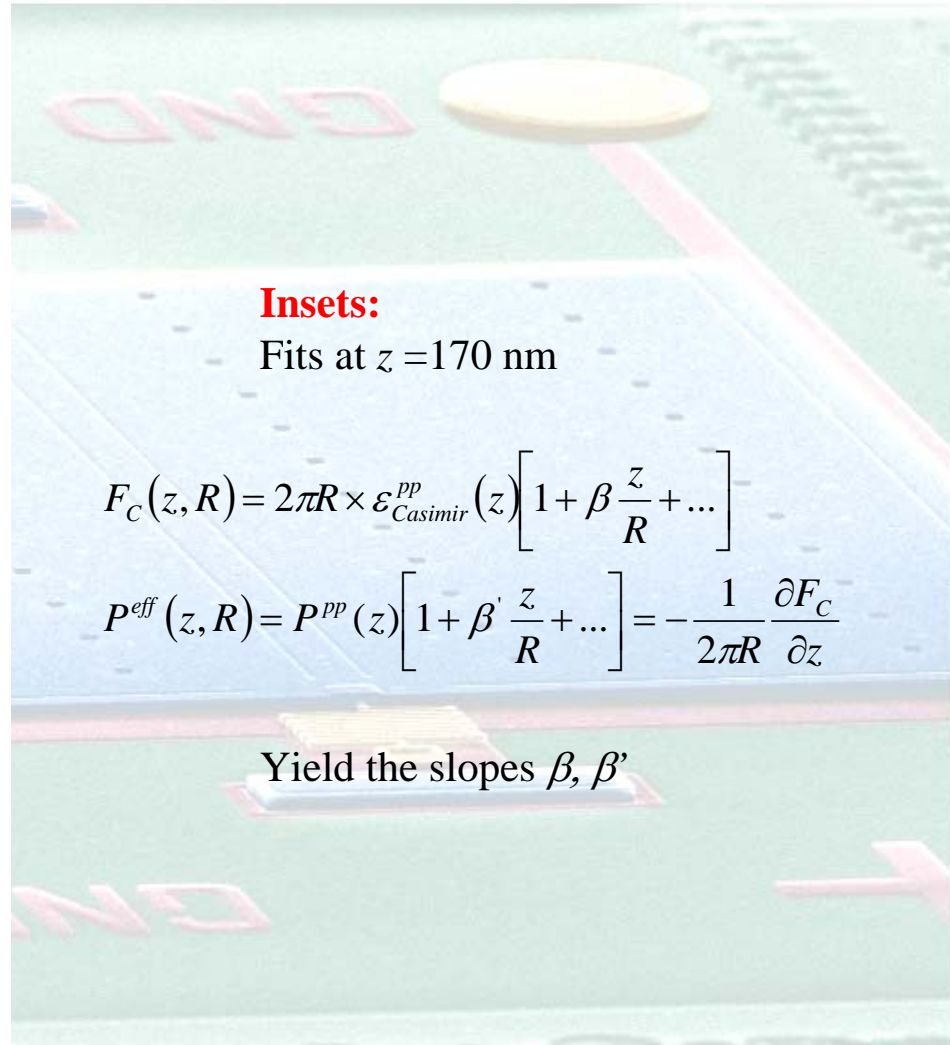
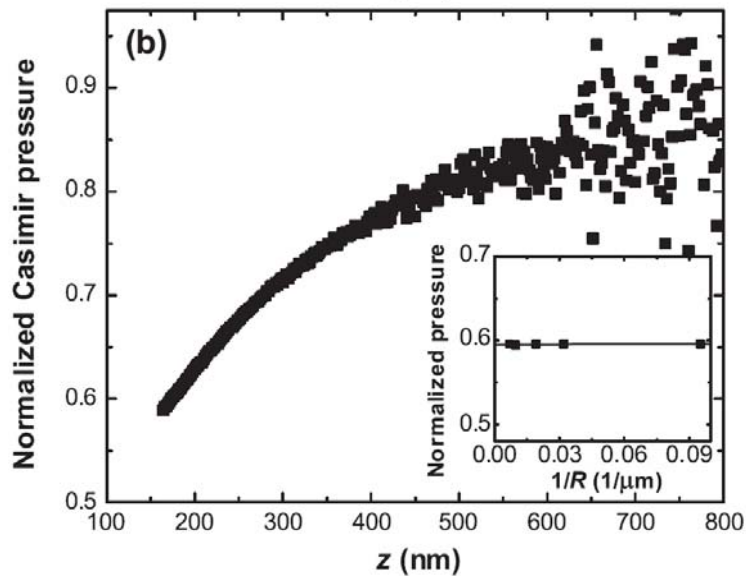
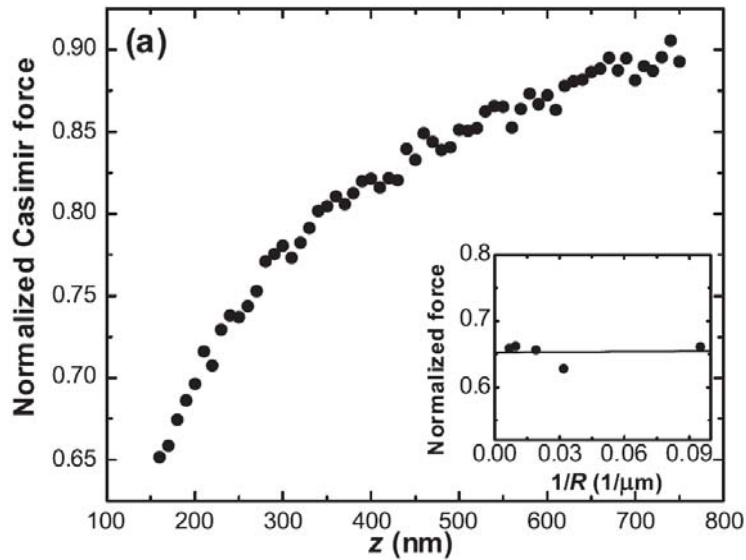
Measurements as a function of R

- 10.5 μm
- 31.4 μm
- 52.3 μm
- 102.8 μm
- 148.2 μm



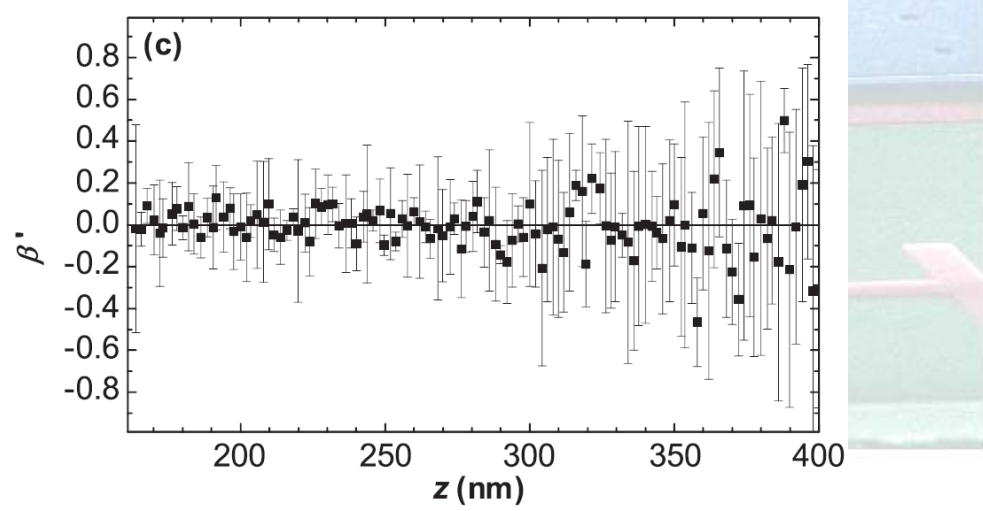
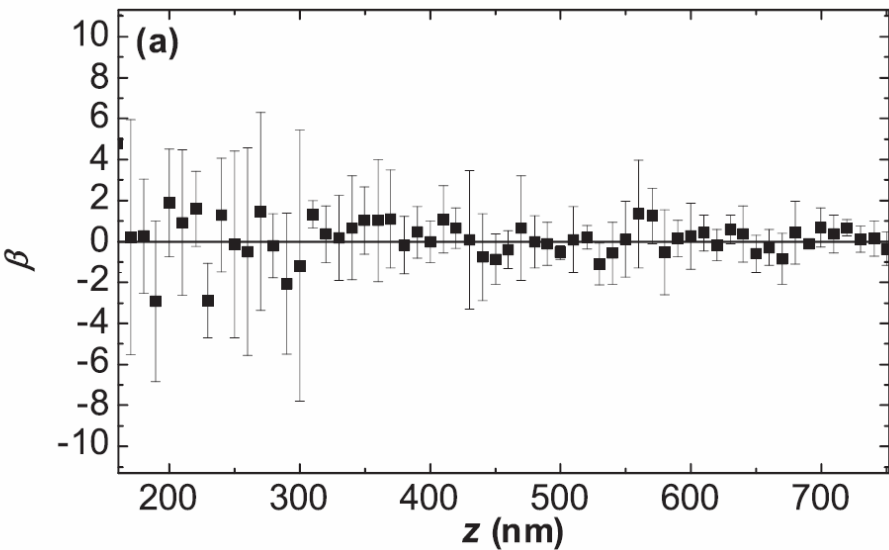
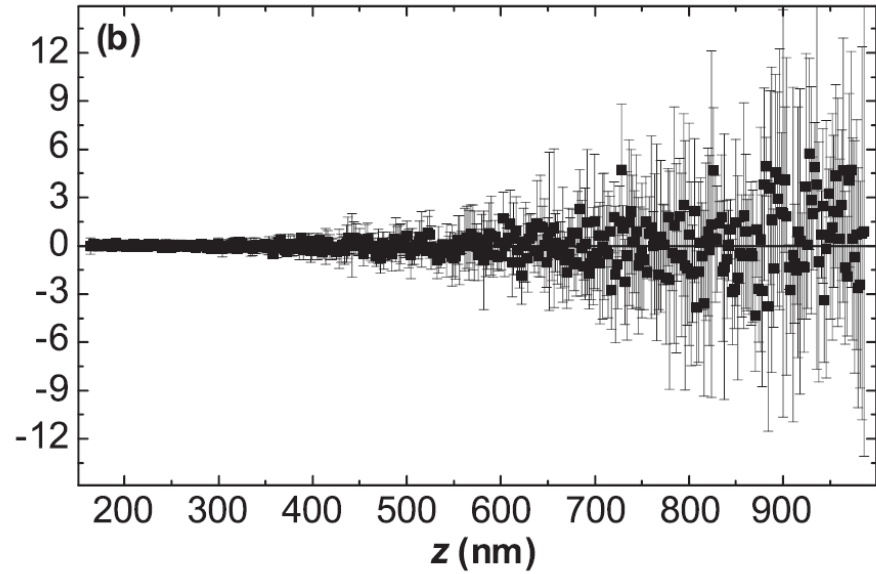
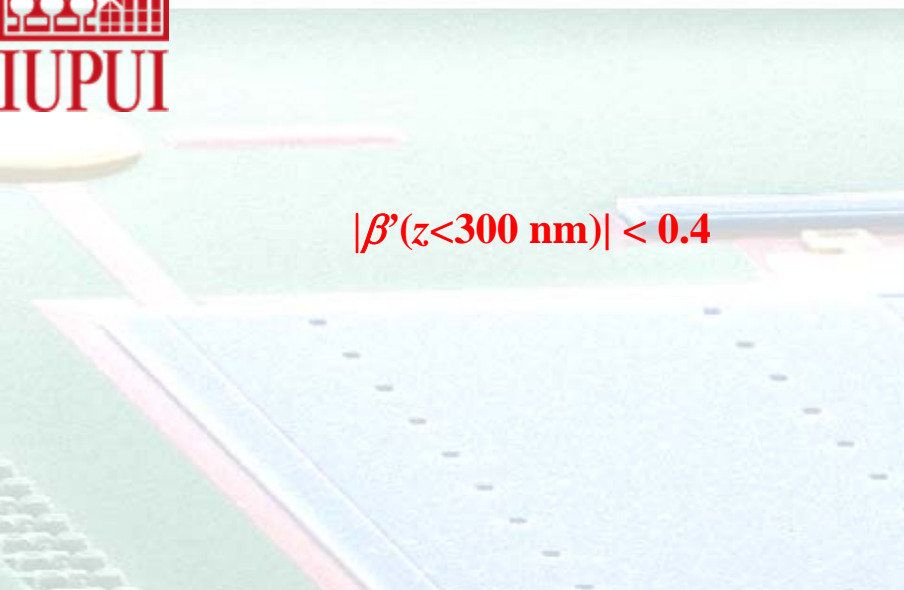


Proximity force approximation





Proximity force approximation





Summary

- **Precise measurement of the Casimir force, with random errors smaller than systematic ones**

This system cannot be used as is to improve on the sensitivity in P_C

- **Good agreement with plasma model**

Differences with Drude model **cannot** be explained as a problem in the separation measurement. It appears that any model with a finite relaxation time will give discrepancies when comparing with the Casimir force.

The Casimir measurements are an effective measurement of the Casimir interaction dependence on T .

- **Preliminary data on temperature dependence**

Significant noise sources. Main suspects: Mechanical coupling and interferometer variations. In consequence the data agree within the experimental error with both the Drude and generalized plasma models.

- **Proximity force approximation**

Experimentally determined the coefficients for the first order in the z/R expansions